Available online at www.sciencedirect.com
SCIENCE DIRECT®
Advances in Space Research xxx (2006) xxx–xxx
ADVANCES IN SPACE RESEARCH (a COSPAR publication)
www.elsevier.com/locate/asr

Petrologic mapping of the Moon using Fe, Mg, and Al abundances

A.A. Berezhnoy [a,*], N. Hasebe [a], M. Kobayashi [a], G. Michael [b], N. Yamashita [a]

[a] Advanced Research Institute for Science and Engineering, Waseda University, 3-4-1 Okubo, Shinjuku-ku, 169-8555 Tokyo, Japan
[b] German Aerospace Centre, Institute for Planetary Research, Rutherfordstr. 2, 12489 Berlin-Adlershof, Germany

Received 16 August 2004; received in revised form 27 January 2005; accepted 1 March 2005

Abstract

A comparison between the abundances of major elements on the Moon determined by Lunar Prospector gamma ray spectrometer and those in returned lunar samples is performed. Lunar Prospector shows higher Mg and Al content and lower Si content in western maria in comparison with the lunar sample collection. Lunar Prospector overestimated the Mg content by about 20%. There are no elemental anomalies at the lunar poles: this is additional evidence for the presence of polar lunar hydrogen. Using Mg, Fe, and Al abundances, petrologic maps containing information about the abundances of ferroan anorthosites, mare basalts, and Mg-rich rocks are derived. This approach is useful for searching for cryptomaria and Mg-rich rocks deposits on the lunar surface. A search is implemented for rare rock types (dunites and pyroclastic deposits). Ca-rich, Al-low small-area anomalies are detected in the far side highlands.

Keywords: Moon; Maps of elemental abundances; Petrology; End-member rocks; Chemistry of lunar polar regions; Rock type identification

1. Introduction

Elemental mapping of the lunar surface is a very useful technique for studying petrologic provinces on the Moon, for searching for chemically anomalous sites and ancient cryptomaria, and for identification of lunar rock types. Using Clementine optical photometric images Lucey et al. (2000) determined FeO and TiO_2 abundances with 100 m spatial resolution within an error of 1 wt%. Such high-resolution data are very useful for the study pyroclastic deposits, central peaks of big craters, and former lava flows. Gamma ray spectroscopy allows estimation of the abundances of many elements at 30–50 cm depth layer on the lunar surface. The spatial resolution of gamma ray spectroscopy of the Moon is limited by the spacecraft altitude above the Moon and equal to about 40 km for Th and Fe as elements with strongest gamma ray lines and to 150 km for Mg and Al for the case of Lunar Prospector data set. The quality of these data is strongly depends on counting statistics and accuracy of calibration technique. Now the full analysis of Fe and Th data as elements with strongest gamma ray lines is finished (Lawrence et al., 2002, 2003, and references therein). Low spectral resolution of this data set is not high enough for avoiding of interference problems of nearest gamma ray lines of different elements. Preliminary data about the abundances of other elements such as O, Si, Mg, Ca, Al, K, U, and Ti are presented by Prettyman et al. (2002).

In this paper we try to analyze the quality of Lunar Prospector gamma ray spectrometer data comparing Lunar Prospector measurements with studies of elemental composition of returned samples. The other goal of our paper is a petrologic mapping of the Moon. Using Apollo gamma ray and X-ray spectrometers data such

* Corresponding author. Present address: Now at Department of Lunar and Planetary Research, Sternberg Astronomical Institute, Moscow State University, Universitetskij pr., 13, 119992 Moscow, Russia. Tel.: +7 095 939 1029; fax: +7 095 932 8841.
E-mail address: a_tolok@mail.ru (A.A. Berezhnoy).

0273-1177/$30
doi:10.1016/j.asr.2005.03.007

as Fe and Th content and Al/Si, Mg/Si ratios, Davis and Spudis (1985) proposed that all observed elemental abundances on the Moon can be explained by the presence of three end members: ferroan anorthosite, mare basalts, and KREEP. In this paper Th content was used for distinction between Mg-suite rocks and KREEP basalts. In our article we develop the three end member hypothesis, using Mg, Al, and Fe Lunar Prospector data and Mg–Fe, Mg–Al petrologic techniques. We do not use Th in our petrologic mapping, because Th Lunar Prospector data were already used in such mapping by Spudis et al. (2000).

2. Accuracy of Lunar Prospector elemental data

Let us estimate the quality of the Lunar Prospector gamma ray spectrometer data by comparing the elemental composition of landing sites measured by Lunar Prospector and by analysis of returned samples. The validity of such an approach was confirmed by Jolliff (1999). In this paper the difference of FeO content at Apollo 17 landing site between Clementine spectral reflectance data and Apollo returned samples data is equal to 0.5 wt%. Although spatial resolution of gamma ray technique cannot achieve so good spatial resolution as the optical technique, this approach can be used even at 150 km spatial resolution data. Let us note that comparison of Lunar Prospector gamma ray spectrometer data with ground truth sample data must be done with caution, because sample sites cover a small area (less than a few kilometers in linear distance), while the footprint size is 150 km for most of the Lunar Prospector gamma ray spectrometer data. There is no guarantee that the small-area measurements from the sample are representative of the large area measurement of the Lunar Prospector gamma ray spectrometer data. The correlation coefficients and standard deviations between both data sets are equal to 0.69 and 1 wt%, 0.66 and 2.9 wt% for Ti and Fe, respectively. The bulk composition of returned samples sites is taken according to Elphic et al. (2000). Usage of the bulk composition of returned samples sites may cause some problems, because some samples might be more representative than others (Vaniman et al., 2002).

But for other elements with weaker gamma ray lines the agreement between both data sets is not so good. The correlation coefficients and standard deviations are equal to 0.49 and 1.6 wt%, 0.32 and 1.5 wt%, 0.24 and 2.2 wt%, 0.13 and 3.2 wt%, −0.64 and 3.5 wt% for Mg, O, Ca, Al, Si, respectively. Variations of O content in different rock types are so small that the accuracy of Lunar Prospector measurements is not enough even for a qualitative analysis of O content. Si Lunar Prospector data contradict the Si content in returned samples. The Si content according to Lunar Prospector results is lower by 5–10 wt% than that measured in returned samples at Apollo 12, 14, 15 sites. Underestimation of Si content leads to Mg and Al content overestimation by some weight percent in Th-rich western maria. Lunar Prospector measures Mg content as 20% higher than that in returned samples (see Fig. 1). The agreement between Lunar Prospector data and returned samples analysis results for Al (see Fig. 2) and Ca content is not good, but becomes better at Al > 8 wt%.

Another way to estimate the quality of Lunar Prospector data is to compare correlations between elemental abundances in the returned sample collection and those according to remote sensing measurements. Study of correlations between Th content and fast neutron flux is useful for detection of ancient impact basins (Gasnault et al., 2002). Correlations between Ca, Al, Mg with Fe and Th are not strong enough for the construction of high-resolution maps for these elements, based on available high-resolution Fe and Th maps. On the other hand these correlations agree well with the returned samples composition. This means that the quality of Lunar Prospector Ca, Al, and Mg data is suitable for qualitative analysis. However, Lunar Prospector Si abundance does not agree with that in returned lunar

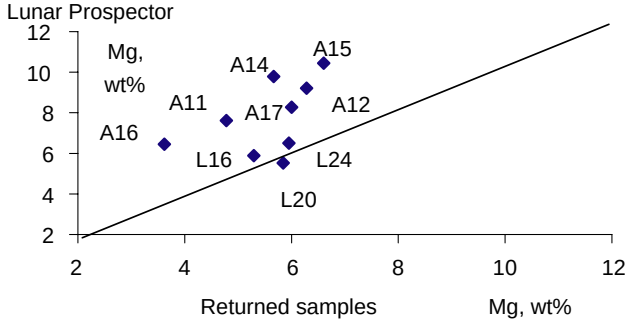

Fig. 1. Comparison between Lunar Prospector measurements of elemental composition of returned sample sites and bulk elemental abundances of returned samples for Mg content.

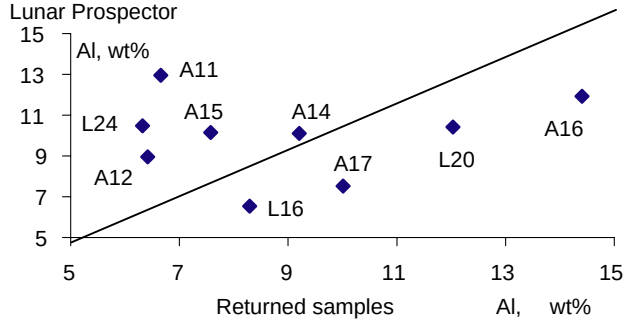

Fig. 2. Comparison between Lunar Prospector measurements of elemental composition of returned sample sites and bulk elemental abundances of returned samples for Al content.

samples. For example, Si–Ti, Si–Th, and Si–Fe data show positive correlations in returned samples (Heiken et al., 1991), but negative correlations in Lunar Prospector data (see Eq. (1)). It may be explained by incorrect calculations by Prettyman et al. (2002) of the partial intensity of Si line at 1779 keV and Mg line at 1369 keV due to interference problems with the strong K line at 1462 keV and the U 1764 keV line. Assuming that Si and Th contents are independent on the lunar surface Si corrected map can be constructed with usage of Eq. (2). The same correction can be conducted for Mg and Al content in Th-rich regions.

$$\mathrm{Si\ (wt\%)} = -0.92^{*}\mathrm{Th\ (ppm)} + 21.2, \quad r^2 = 0.65, \quad \sigma = 1.2\ \mathrm{wt\%} \tag{1}$$

$$\mathrm{Si\ (corrected, wt\%)} = \mathrm{Si\ (old, wt\%)} + 0.92^{*}\mathrm{Th\ (ppm)} \tag{2}$$

3. Chemistry of polar regions of the Moon

One of the most exciting controversies of lunar science is the presence of volatiles at the lunar poles (Feldman et al., 2002; Cocks et al., 2002; Crider and Vondrak, 2003; Berezhnoy et al., 2003). Studying neutron spectra in the polar lunar regions, Feldman et al. (1998) proposed that the decrease of epithermal neutron flux over poles may be explained by the presence of hydrogen in the form of water ice. For the best explanation of observations water ice mass fraction of about 1.5 wt% is indispensable in the south polar caps (Feldman et al., 2000). However, other interpretation of the observations is possible. Hodges (2002) proposed that the observable data can be explained by the presence of regolith with an unusual elemental composition. Namely, CaO content must be lower than 10 wt% or SiO_2 content must be higher than 60 wt% at the poles of the Moon.

The Si Lunar Prospector content is maximal in the highlands, the maximal value being 24.6 wt%, which corresponds to about 53 wt% SiO_2 content. The maximal Si content is 22.3 wt% in lunar polar regions (72.5–90°). This value is too low for significant changes of epithermal neutron flux. The Si content at both poles (87.5–90°) does not differ from that at neighboring locations. Minimal Ca abundances as low as 2 wt% are detected at a few 150-km pixels at lunar maria. The minimal Ca abundance in the lunar polar regions located in highlands (72.5–90°) is 9 wt%, which corresponds to CaO content equal to 13 wt%. The Ca content at both poles (87.5–90°) is equal to 11.5 wt% and does not differ from that at neighboring locations. Thus, Lunar Prospector data do not support the hypothesis of Hodges (2002), at least at 150 km resolution and available statistical accuracy of the data. More detailed study of Hodges hypothesis can be conducted when the spatial resolution of Ca and Si maps will be comparable with the size of permanently shaded craters. This means that the hydrogen hypothesis for explanation of neutron flux changes over the lunar poles is the preferred one.

4. Petrologic mapping of the Moon

Using Al–Mg-number/Th/Ti ratio normalized to chondrites and Mg-number–Th/Ti ratio normalized to chondrites diagrams, Davis and Spudis (1985) estimated abundances of main pristine rock types such as KREEP basalts, mare basalts, and ferroan anorthosites in equatorial lunar regions assuming that all sets of possible elemental compositions of the lunar regolith can be explained by mixture of these three end member rock types. In our work we choose Mg–Al and Mg–Fe diagrams and mare basalts, ferroan anorthosites, and Mg-rich rocks as end members. The use of these diagrams has some advantages in comparison with previously used diagrams, because the two-element approach eliminates the errors resulting from dividing numbers that can have high uncertainties. Let us assume that ferroan anorthosites contain 0.5 wt% Mg, 18 wt% Al, 1 wt% Fe, mare basalts contain 5 wt% Mg, 5 wt% Al, 16 wt% Fe,

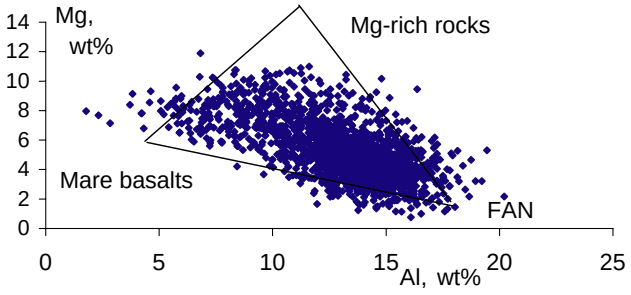

Fig. 3. Scattergram shows Lunar Prospector gamma-ray spectrometer data for 5° squares in Mg–Al compositional space. Elemental composition of three end members is also given.

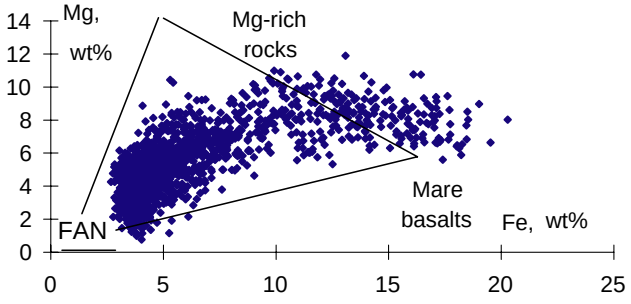

Fig. 4. Scattergram shows Lunar Prospector gamma-ray spectrometer data for 5° squares in Mg–Fe compositional space. Elemental composition of three end members is also given.

and Mg-rich rocks have a composition similar to that of troctolites containing 14 wt% Mg, 12 wt% Al, 5 wt% Fe according to Phillips (1986). Then the relative abundances of end members were determined for each pixel on the lunar surface. Primary colors red, blue, and green are assigned for the end member classes of mare basalts, ferroan anorthosites, and Mg-rich rocks, respectively. The ternary space defined by these points is represented by the mixture of these primary colors.

Majority of the lunar surface belongs to highlands with ferroan anorthosite as the dominant rock type (see Figs. 3 and 4). Mg-rich rocks are located in some cryptomaria such as Copernicus cryptomare and the Balmer basin, in Mare Frigoris and the Gartner-Atlas regions, at the edges of big maria, and east from Mare Serenitatis. Let us note that the abundance of Mg-rich rocks may be overestimated due to overestimation of the Mg content by Lunar Prospector. The presence of mare basalts in the highlands is detected in the majority of known cryptomaria: the Lomonosov-Fleming basin, the Schillerd-Schickard and Mendel-Rydberg regions, and in Mare Orientale. Our results agree well with the petrologic mapping of the Moon conducted by Spudis et al. (2000). This demonstrates the suitability of our approach for representing lunar petrologic provinces.

It is possible to search for rare rock types, based on Lunar Prospector data. The elemental composition of rare rock types is taken from Phillips (1986). The size of the biggest pyroclastic deposit region at the Aristarchus plateau is comparable with Lunar Prospector footprint. This region can be distinguished from surrounding places by unusually high Mg/Al ratio (1.4), and by high Th (6.5 ppm) and Ti (3.2 wt%) content. Other pyroclastic deposits are too small for detection at 150 km spatial resolution. The search for dunite deposits (25 wt% Mg, 1 wt% Ca, 1 wt% Al) was unsuccessful at the scale of Lunar Prospector gamma ray spectrometer. While we choose troctolites as a third end-member, there are no regions on the Moon with elemental composition typical for troctolites. But other Mg-rich rock types were detected. Gabbronorites are located at the edges of eastern maria. It is difficult to distinguish norites, because norites have almost the same Mg, Fe, and Al abundances as the mixture of ferroan anorthosites and troctolites.

There are Ca-rich, Al-poor anomalies in the far side highlands (for example, at 45°N, 130°E and 35°N, 133°W). The size of these anomalies is less than 150 km, because they occur as one-pixel anomalies on Lunar Prospector elemental maps. Such regions have higher Ca (14–17 wt%) and Fe (~4 wt%) content, lower Al (10–12 wt%) content in comparison with surrounding areas. These data show the existence of a Ca-rich rock type.

If the three end-member hypothesis is correct and errors of measurements are negligible, then the abundances of end-members in each pixel, determined by Mg–Fe and Mg–Al approaches, should be the same. However, the abundances of end members determined by Mg–Al and Mg–Fe contents are different (see Figs. 3 and 4) due to the presence of rocks with different elemental composition from the end-member rocks and due to existence of errors of estimation of elemental abundances. Future goal is to study Lunar Prospector data in Mg–Al–Fe space. When more accurate elemental abundances data will be available, it will be possible to add KREEP basalts as fourth end-member.

5. Conclusions

Comparison of elemental composition at landing sites between Lunar Prospector and returned samples is a good method to estimate the quality of Lunar Prospector gamma-ray spectrometer data despite the differences in resolution and techniques. Lunar Prospector O and Si data are not suitable for data analysis. Lunar Prospector overestimates the Mg content relatively to samples, especially for western maria.

Polar lunar regions have almost the same elemental composition as those at surrounding places. These results contradict the hypothesis of Hodges (2002) that Ca polar anomalies may be responsible for the variation of neutron flux over the lunar poles. This is an additional confirmation of the presence of hydrogen at the poles of the Moon. Petrologic mapping of the Moon, using Fe, Mg, and Al content, is a powerful method for estimation of the abundances of ferroan anorthosites, mare basalts, and Mg-rich rocks on the lunar surface. For example, gabbronorites are detected at the edges of eastern maria. Ca-rich, Al-poor anomalies are detected in far side highlands. The Lunar Prospector gamma ray spectrometer data appears to be useful for analysis of elemental composition of the lunar surface. Some limitations are pointed out due to problems of interfering gamma ray lines at low spectral resolution.

In the near future our knowledge about elemental composition of the lunar regolith will be greatly improved. The SMART-1 X-ray spectrometer will start to map Al, Mg, Fe, and Si abundances on the Moon in 2005 (Dunkin et al., 2003). The SELENE gamma ray spectrometer, employing a Ge detector with excellent energy resolution, will determine the abundances of main elements on the Moon (Kobayashi et al., 2002).

Acknowledgments

A.A. Berezhnoy is supported by a postdoctoral fellowship grant (No. P02059), provided by the Japanese Society for the Promotion of Science (JSPS). G. Michael acknowledges the financial support provided through the European Community's Human Potential Pro-

gramme under contract RTN2-2001-00414, MAGE. We acknowledge two anonymous referees: their remarks helped us to improve this paper.

References

Berezhnoy, A.A., Hasebe, N., Hiramoto, T., et al. Possibility of the presence of S, SO_2, and CO_2 at the poles of the Moon. Publ. Astron. Soc. Jpn. 55, 859–870, 2003.

Cocks, F.H., Klenk, P.A., Watkins, S.A., et al. Lunar ice: adsorbed water on subsurface polar dust. Icarus 160, 386–397, 2002.

Crider, D.H., Vondrak, R.R. Space weathering effects on lunar cold trap deposits. J. Geophys. Res. 108, 2003, pp. 15-1, CiteID 5079.

Davis, P.A., Spudis, P.D. Petrologic province maps of the lunar highlands derived from orbital geochemical data. J. Geophys. Res. 90, D61–D74, 1985.

Dunkin, S.K., Grande, M., Casanova, I., et al. Scientific rationale for the D-CIXS X-ray spectrometer on board ESA's SMART-1 mission to the Moon. Planet. Space Sci. 51, 435–442, 2003.

Elphic, R.C., Lawrence, D.J., Feldman, W.C., et al. Lunar rare earth element distribution and ramifications for FeO and TiO_2: Lunar Prospector neutron spectrometer observations. J. Geophys. Res. 105, 20333–20345, 2000.

Feldman, W.C., Maurice, S., Binder, A.B., et al. Fluxes of fast and epithermal neutrons from Lunar Prospector: evidence for water ice at the lunar poles. Science 281, 1496–1500, 1998.

Feldman, W.C., Lawrence, D.J., Elphic, R.C., et al. Polar hydrogen deposits on the Moon. J. Geophys. Res. 105, 4175–4196, 2000.

Feldman, W.C., Maurice, S., Lawrence, D.J., et al. Evidence for water ice near the lunar poles. J. Geophys. Res. 106, 23231–23252, 2002.

Gasnault, O., Feldman, W.C., d'Uston, C., et al. Statistical analysis of thorium and fast neutron data at the lunar surface. J. Geophys. Res. 107 (E10), 2002, pp. 2-1, CiteID 5072.

Heiken, G.H., Vaniman, D.T., French, B.M. Lunar Sourcebook. Cambridge University Press, Houston, TX, USA, 1991.

Hodges, R.R. Reanalysis of Lunar Prospector neutron spectrometer observations over the lunar poles. J. Geophys. Res. 107, 2002, pp. 8-1, CiteID 5125.

Jolliff, B.L. Clementine UV–VIS multispectral data and the Apollo 17 landing site: what can we tell and how well? J. Geophys. Res. 104, 14123–14148, 1999.

Kobayashi, M., Fujii, M., Hasebe, N., et al. High-purity germanium gamma ray spectrometer with Stirling cycle cryocooler. Adv. Space Res. 30, 1927–1931, 2002.

Lawrence, D.J., Feldman, W.C., Elphic, R.C., et al. Iron abundances on the lunar surface as measured by the Lunar Prospector gamma-ray and neutron spectrometers. J. Geophys. Res. 107 (E12), 2002, 13-1, CiteID 5130.

Lawrence, D.J., Elphic, R.C., Feldman, W.C., et al. Small-area thorium features on the lunar surface. J. Geophys. Res. 108 (E9), 2003, 16-1, CiteID 5102.

Lucey, P.G., Blewett, D.T., Jolliff, B.L. Lunar iron and titanium abundance algorithms based on final processing of Clementine ultraviolet–visible images. J. Geophys. Res. 105, 20297–20306, 2000.

Phillips, R. (Ed.). LGO Science Workshop, Contributions of a Lunar Geoscience Observer Mission to Fundamental Questions in Lunar Science, Department of Geological Sciences, Southern Methodist University, Dallas, TX, 1986.

Prettyman, T.H., Feldman, W.C., Lawrence, D.J., et al. Library least square analysis of Lunar Prospector gamma-ray spectra, Abstract No. 2012, in: Presented at 33rd Lunar and Planetary Science Conference, Houston, USA, March, 2002.

Spudis, P.D., Bussey, D.B.J., Gillis, J.J. Petrologic mapping of the Moon from Clementine and Lunar Prospector data: Incorporation of new thorium data, Abstract No. 1414, in: Presented at 31st Lunar and Planetary Science Conference, Houston, USA, March, 2000.

Vaniman, D., Lawrence, D., Gasnault, O., et al. Extending the Th–FeO sampling range at Apollo 14: under the footprint of Lunar Prospector, Abstract No. 1404, in: Presented at 33rd Lunar and Planetary Science Conference, Houston, USA, March, 2002.